Influence of Added Electrolytes on the Lyotropic Phase Behavior of Triethylammoniodecyloxycyanobiphenyl Bromide (OCB-$C_{10}NEt_3Br$)

G. S. Attard,[†] S. Fuller,[‡,§] and G. J. T. Tiddy*[,‡,§]

Department of Chemistry, University of Southampton, Southampton, U.K., Department of Pure and Applied Chemistry, University of Salford, Salford, U.K., and Department of Chemical Engineering, UMIST, PO Box 88, Manchester M60 1QD, U.K.

Received: April 7, 2000; In Final Form: August 15, 2000

The influence of added electrolytes (NaBr, NaCl, Na_2SO_4, Na_3PO_4, Na_2HPO_4, NaSCN) on the lyotropic mesophase behavior of triethylammoniodecyloxycyanobipenyl bromide (OCB-$C_{10}NEt_3$) has been studied using optical microscopy, X-ray diffraction, and NMR. Optical microscopy was employed to map the existence regions of the lamellar mesophase, while X-ray diffraction gave its interaggregate dimensions, and NMR was employed to monitor water ordering. Only lamellar and micellar phases have been observed. In all of the electrolytes except NaSCN, partial miscibility of surfactant and water is induced above a certain concentration. This usually involves the separation of a dilute surfactant solution from a more concentrated one. It does not occur *within* the extensive lamellar phase region. X-ray diffraction and NMR results demonstrate that the major influence of the electrolytes is to reduce the area per headgroup within the aggregates. The effects of the electrolytes follow the Hofmeister series and are attributed to adsorption or desorption of anions at the aggregate surface rather than to changes in "water structure". Sodium thiocyanate causes the occurrence of a "re-entrant" isotropic phase, in part because the lamellar phase is stabilized to low concentrations. The displacement of OCB groups from the micellar surface by SCN ions is suggested to account for this, which, if valid, offers a potential route to obtaining *true amphitropic mesophases* (i.e., materials with both thermotropic and lyotropic liquid crystalline order).

Introduction

Recently, there has been interest in a novel class of materials which can exhibit both lyotropic and thermotropic memomorphism, the so-called *amphitropic* mesogens.[1−11] The dual mesomorphism arises because of their hybrid molecular structure, where a typical surfactant polar headgroup (e.g., quarternary ammonium, or oligoethylene glycol group) is attached to a thermotropic mesogenic moiety such as a rodlike dipolar unit (e.g., cyanobiphenyl) via a methylene chain. A consequence of this hybrid molecular structure is that the micellar aggregation behavior is modulated by the anisotropic dispersion and packing interactions of the rodlike dipolar units. These systems are of considerable interest because they offer the possibility of combining surfactant mesomorphism with the mesomorphism of conventional thermotropic systems. In order to determine the influence of the various interactions involved, we have undertaken a systematic study of mixtures of both standard thermotropic and lyotropic mesogens, and of the novel surfactants where the two parts are chemically joined together.

In an earlier paper[3] we reported on the mesophases formed by a conventional surfactant (octaethylene glycol hexadecyl ether, $C_{16}EO_8$) with an added thermotropic mesogen, pentylcyanobiphenyl (5-CB). Then we examined compounds where the thermotropic mesogenic group, a cyanobiphenyl moiety, was chemically attached to the surfactant hydrophobic chain.[5] There have already been reports on other similar single chain materials[6−10] with different headgroups, and on double chain quaternary ammonium compounds.[11] Everaars et al. report[11] on a series of compounds containing a single quaternary ammonium ion connected to two alkyl chains with terminal cyanobiphenyl groups. We have studied both conventional single chain amphitropic surfactants, and *gemini* amphitropic surfactants. (Gemini surfactants are materials where two conventional surfactant molecules are joined together by a spacer of variable length, in our case, up to C_6 alkyl moieties.) In a previous paper[5] we compared the lyotropic behavior of a series of gemini surfactants having chain-terminal oxycyanobiphenyl (OCB) moieties with that of the normal "gemini" surfactants. The OCB unit was separated from the headgroup by an alkyl group spacer of varying length (4−6 CH_2 groups). The major influence of the attached OCB was to favor a lamellar (L_α) phase over hexagonal (H_1) and bicontinuous cubic (V_1) phases that are formed with normal surfactants. Very unusually,[4,5] we observed two coexisting lamellar phases having different water contents in the binary surfactant−water system, which might have been an indication of unusual mesophase structures. However, the two lamellar phases were not present with a *single* chain surfactant having an OCB unit attached to a $(CH_2)_{10}$ spacer,[4] which gave a large lamellar phase region. Again the OCB unit had destabilized the hexagonal and bicontinuous cubic phases which occur with the equivalent conventional surfactant. The coexistence of the two lamellar phases we now believe to be associated with specific counterion binding of bromide ions in gemini (and other) surfactants[12] rather than any influence of the OCB (see below).

More recently,[13] we have reported further studies on this single chain amphitropic surfactant, 10-(4′-cyano-4-biphenyloxy)decyltriethyammonium bromide (OCB-$C_{10}NEt_3$). Note that

[†] University of Southampton.
[‡] University of Salford.
[§] UMIST.

10.1021/jp0013513 CCC: $19.00
Published on Web 10/14/2000

the effect on the mesophase structures of the triethylammonium group rather than a trimethylammonium group has been established to be small.[4,14] For example, both the hexadecyl derivatives form hexagonal, bicontinuous cubic, and lamellar phases. We demonstrated that added cyanbiphenyl thermotropic mesogens stabilize the lamellar phase, while hexane destabilizes it. Also, NMR and X-ray measurements suggested that, at high water concentrations, the surfactant aggregates of the lamellar phase contained water-filled defects, similar to the structures found in the lamellar phase of fluorocarbon soaps and longer chain nonionic surfactants systems.[15−21] In order to investigate the properties of these unusual surfactants further, we have examined the changes caused by added electrolytes. Our intention was to discover if it was possible to induce the two lamellar phase coexistence (observed for the "gemini" amphitropic surfactants)[4] by adding electrolytes with counterions that adsorb to the surfactant aggregates ("salting-in systems").

The influence of added electrolytes on surfactant phase behavior has been studied over many years, with the work of McBain[22−4] providing a firm basis for others to build on. McBain and co-workers demonstrated that high levels of electrolytes (ca. 1−2 mol dm^{-3} sodium and potassium chlorides) caused the (almost) continuous miscibility of water and surfactant through solution and liquid crystal phases (forming micellar solution (L_1), hexagonal, cubic/intermediate and lamellar phases) to be replaced by dilute surfactant monomer solution, L_1 and L_α, phases with several pronounced miscibility gaps. The first is the separation of a micellar solution from a very dilute surfactant solution (W) with electrolyte, and the second involves the separation of the lamellar phase, from either L_1 or W according to electrolyte concentration. The first process resembles the behavior of polyoxyethylene surfactants above their "cloud point (temperature)" where dilute and concentrated solutions phase-separate. (This is termed the cloud point because the solutions turn cloudy.) In ionic surfactants these changes can be understood by considering two factors. First, the electrolyte reduces the area per surfactant headgroup within micelles because (partly) of reduced electrostatic repulsion, thus giving aggregates of smaller curvatures. Second, the electrolyte results in the occurrence of a net attractive interaction between the aggregates, leading to phase separation. It is likely that the micelles in the L_1 phase that separate first have some *flat-plate* character (i.e., they are a type of disk micelle (but not circular disks),[25] as this often produces larger net attractive forces than occurs with the spherical or rod micelles. Clearly, there is *flat-plate* character to the attractive forces that cause the separation of the lamellar phase. The induction of partial miscibility in ionic surfactant/water mixtures by added electrolytes appears to be a common phenomenon, although an extensive range of surfactant compositions is often not examined. It resembles the electrolyte-induced precipitation of proteins from aqueous solution, where the efficacy of various types is represented by the well-known Hofmeister series, some increasing solubility ("salting-in") while others reduce solubility ("salting-out"). Because the anions dominate behavior, it might be expected that large differences between different electrolytes would be observed with cationic surfactants. For this reason, and because of the unusual lameller structure in this system, together with the relatively low Krafft boundary and the possibility of observing lamellar/lamellar coexistence, we have examined the influence of a range of electrolytes on OCB-$C_{10}NEt_3$. The electrolytes chosen span the Hofmeister series (salting-in: sodium thiocyanate, bromide; indifferent: sodium chloride; and salting-out: sodium phosphates, sulfate).

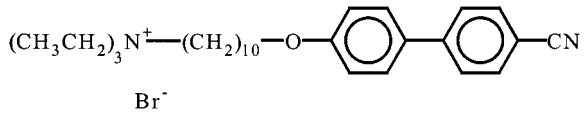

Figure 1. Structure of 10-(4′-cyano-4-biphenyloxy)decyltriethylammonium bromide (OCB-$C_{10}NEt_3$).

We have employed a range of techniques in the investigation. First, an initial survey of the phase behavior as a function of electrolyte concentration was made using the Lawrence penetration scan with polarizing microscopy.[26,27] Then, for some selected electrolytes, the bulk phase behavior was determined for individual samples, again using microscopy but also with observations by eye. Following this, several systems were selected for more detailed investigation using NMR and X-ray diffraction to monitor the detailed structural changes induced in the surfactant aggregates. The results show that electrolytes easily induce partial miscibility in this system, but always involving at least one isotropic phase. It would appear that the presence of ethyl rather than methyl groups on the nitrogen is a factor in preventing the observation of two coexisting lamellar phases, although it does not significantly alter the types of phases formed.

Experimental Section

Materials. 10-(4′-Cyano-4-biphenyloxy)decyltriethylammonium bromide (OCB-$C_{10}NEt_3$) was synthesized as reported previousely.[4] 4-Hydroxy-4′-cyanobiphenyl was coupled with α,ω-dibromodecane to give α-bromodecyl-ω-4,4′-cyanobiphenyl, which was reacted with excess triethylamine to give OCB-$C_{10}NEt_3$. Purity was established by a single spot on TLC/HPLC and ^1H NMR at 300 MHz. Water was deionized and double distilled. Heavy water (>99.7%) was obtained from Aldrich. All the inorganic electrolytes were the most pure grades commercially available and were used as received.

Methods. Bulk samples were prepared by weighing the constituents into glass tubes which were sealed and the contents mixed by heating and centrifugation. Microscopy was carried out using a Carl Zeiss Jenaval polarizing microscope fitted with a Linkam THM600 hot stage and TMS 90 temperature control unit (accuracy ±0.5 °C). X-ray diffraction measurements were made at the CLRC (then SERC/EPSRC) Daresbury laboratories on stations 7.2 for wide-angle scattering (<100 Å) and 8.2 for small-angle scattering (>60 Å). Calibration was carried out using standard samples provided (silica, graphite, for 7.2, rat-tail collagen for 8.2). NMR measurements (^2H) were made using a Bruker AC 300 MHz spectrometer and variable-temperature probe operating at 46.07 MHz. For NMR measurements the accuracy was typically ±5% or better, while for the X-ray data the errors were ±1−2 Å with d_0 > 100 Å, falling to <1 Å with d_0 < 50 Å.

Results

Microscopy and Optical Studies. (A) Penetration Scans. In the absence of a solvent, OCB-$C_{10}NEt_3$ forms no thermotropic mesophases, but melts to an isotropic liquid at 110 °C. The phase behavior with water (D_2O) is shown in Figure 2, which demonstrates the large region of lamellar phase.[13] An initial survey of behavior was made by contacting OCB-$C_{10}NEt_3$ with the various electrolyte solutions on a microscope slide, placing the sample on the Linkam hot stage and observing the sequence of phases formed as a function of temperature, both on heating and cooling. As supercooling of molten phases is commonplace at the Krafft boundary, most of the transitions reported are those

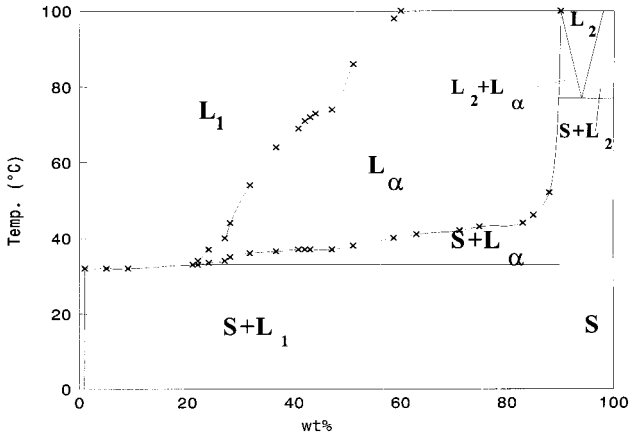

Figure 2. Phase diagram of OCB-$C_{10}NEt_3$ (wt %) with water (^2H_2O), from ref 13. Isotropic solutions: L_1, L_2; lamellar phase: L_α; solid: S. The boundaries of the L_2 "concentrated surfactant liquid" phase were not determined as this region was seen only in penetration scans.

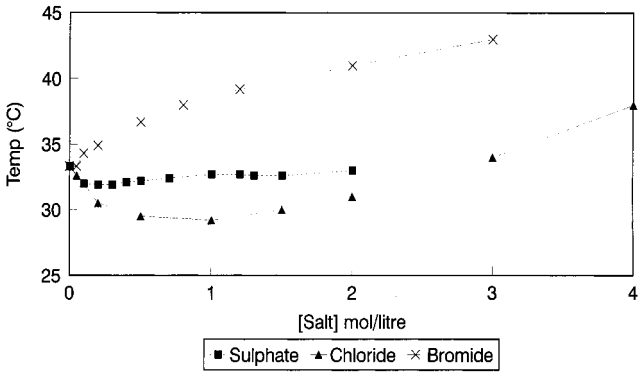

Figure 3. Penetration temperatures for the lamellar phase of OCB_{10}-NEt_3 in sodium salt solutions.

noted on heating scans. The *penetration temperature* (T_{pen}) as used by Lawrence[26,27] is the minimum temperature for the observation of a particular phase.

Penetration scans have been carried out on samples of OCB-$C_{10}NEt_3$ using solutions of sodium bromide, chloride, sulfate, thiocyanate, and phosphates (Na_3PO_4 and Na_2HPO_4) of various concentrations. Note that this is a kinetic experiment where surfactant is continuously dissolving, so the attainment of long-term equilibrium is not possible. Care must be taken to ensure that the concentration gradient really does cover the span from water to surfactant. Also, where a third component is present (e.g., electrolyte) then care must be taken to ensure that the concentration of the third component is that of the initial solution—i.e., the solvent is in excess and does not dry out! In water, the lamellar phase T_{pen} of OCB-$C_{10}NEt_3$ is 33.3 °C, and the lamellar phase occupies a large part of the phase diagram (Figure 2).

Sodium Bromide Solutions. We start with sodium bromide because this has the same cation as the surfactant. For the lamellar phase T_{pen} is increased by solutions of molarity greater than 0.08 mol dm^{-3} and reaches 43 °C in 3 mol dm^{-3} solution (Figure 3). This increase is not that surprising, probably arising from the *common ion* effect which occurs because of the increase in bromide concentration. The separation of dilute and concentrated surfactant solutions ("clouding", or partial miscibility, i.e., the formation of a second micellar phase L_1') does occur. It is first seen at 0.06 mol dm^{-3} and 32 °C, but is not present below this at 0.05 mol dm^{-3}. At this concentration the phase sequence L_1/S changes to L_1/L_1'/S on heating. The clouding is part of a *lower consolute boundary* of a closed partial

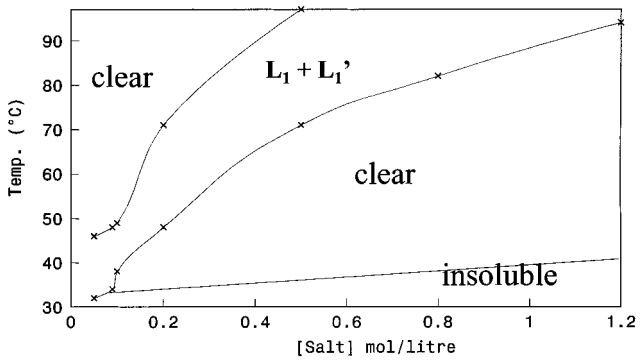

Figure 4. Partial miscibility behavior (temperature range for coexistence of an $L_1 + L_1'$ region as a function of electrolyte concentration) observed by optical microscopy for the aqueous solution region in the OCB-$C_{10}NEt_3$/NaBr system. Clear = single solution (L_1); $L_1 + L_1' =$ two coexisting solutions; insoluble − surfactants below Krafft point. The experimental temperatures measured for the boundary of the region where $L_1 + L_1'$ coexistence is observed are indicated by X.

miscibility loop. The *lower consolute temperature* (LCT) increases with electrolyte concentration, reaching 94 °C at 1.2 mol dm^{-3}. At higher concentrations (up to 3 mol dm^{-3}), if clouding occurs it is above 100 °C. At 0.06 mol dm^{-3} the *upper consolute temperature* (UCT) of the loop (two isotropic phases change to one phase) is observed at 47 °C which increases to 97 °C at 0.5 mol dm^{-3}, and then moves above 100 °C. The occurrence/disappearance of the two isotropic phases as a function of electrolyte level is shown in Figure 4. Between 0.05 and 0.09 mol dm^{-3} NaBr partial miscibility begins at a lower temperature, albeit only 1−1.5 °C, than the lamellar phase. In this region, it appears that clouding occurs at about the Krafft temperature, i.e., that the LCT really lies below the Krafft boundary. Thus, on heating the sample, after "electrolyte penetration", an additional isotropic phase adjacent to the solid surfactant is observed first. On further heating, a band of lamellar phase appears at the edge of the solid. Above this electrolyte concentration the lamellar phase is formed at a lower temperature than the occurrence of clouding (Figure 4). Note that from the penetration experiment it is obvious that a low-temperature (clear) micellar phase does occur at lower concentrations than the lamellar phase. Hence the initial effect of added electrolyte is to induce clouding, but the LCT increases with the addition of more electrolyte ("salting-in"). Whether or not the UCT continues to increase above ca. 0.5 mol dm^{-3} electrolyte was not investigated. No indication of two coexisting lamellar phases was observed, nor does the partial miscibility loop contact the lamellar phase.

Sodium Chloride Solutions. For sodium chloride solutions, T_{pen} initially decreases with increasing electrolyte concentration reaching a minimum of 29.2 °C at 1.0 mol dm^{-3} and then increases to 38 °C at 4.0 mol dm^{-1} (Figure 3). Since cationic alkylammonium chloride surfactant salts usually have lower Krafft temperatures than bromides, we expect this decrease in T_{pen}. Partial miscibility is again observed in the micellar phase region of the penetration scan at surfactant concentrations lower than those needed for the formation of a lamellar phase. The lowest electrolyte concentration at which this is seen is 0.085 mol dm^{-3} NaCl at a LCT of 34.3 °C. No imiscibility is seen at 0.080 mol dm^{-3} NaCl. This temperature decreases to 17 °C at 1.0 mol dm^{-3} before increasing to 94 °C at 3.5 mol dm^{-3}. No L_1' phase is seen at 4.0 mol dm^{-3}. The upper consolute temperature (UCT) increases from 39.0 °C at 0.085 mol dm^{-3} to 93 °C at 2.0 mol dm^{-3}. No remiscibility is seen at 3.0 mol dm^{-3}; i.e., the UCT is above 100 °C (Figure 5).

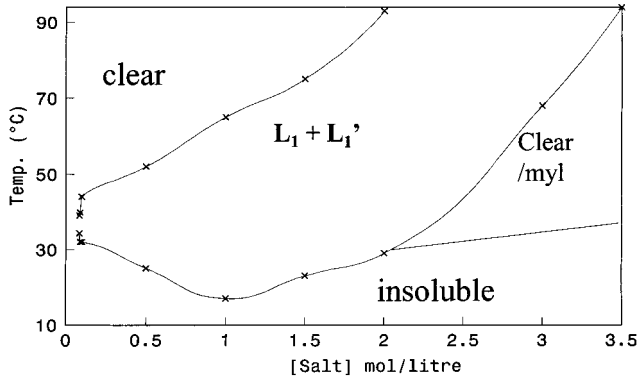

Figure 5. Partial miscibility behavior (temperature range for coexistence of an $L_1 + L_1'$ region as a function of electrolyte concentration) in the OCB-$C_{10}NEt_3$/NaCl system. Labels as for Figure 4; myl indicates possible occurrence of $W + L_\alpha$ region, see text.

At concentrations between 0.1 and ~2 mol dm^{-1}, partial miscibility occurs at about the Krafft temperature, i.e., the LCT really lies below the Krafft boundary. The two isotropic phases are seen before the formation of the lamellar phase (i.e., the phase sequence $L_1/L_1'/S$ (=solid) changes to $L_1/L_1'/L_\alpha/S$ on heating). At a still higher temperature, the clouding disappears to leave a fully isotropic liquid bordering the lamellar phase. Above ~2 mol dm^{-3} NaCl, the lamellar phase is seen before the partial miscibility (i.e., the phase sequence $L_1/L_\alpha/S$ changes to $L_1/L_1'/L_\alpha/S$ on heating). At 4 M NaCl this temperature is above 100 °C. From these observations we see that the initial effect of added salt is to lower the LCT while increasing the UCT.

Again, no indication of two coexisting lamellar phases was observed. Whether or not the partial miscibility loop contacts the lamellar phase is uncertain. From the observations described so far, this certainly is not the case below ca. 2.0 mol dm^{-3} electrolyte. Plate 1a shows the development of the second isotropic phase from dissolution of the solid with 1.0 mol dm^{-3} salt at 25 °C. But for the 3.0 mol dm^{-3} solution, myelins are seen before the second isotropic phase occurs (Plate 1b,c). (Myelins are tubules (ca. 50−300 μm diameter) of lamellar phase that grow from the solid out into the isotropic solution, rather than the usual smooth boundary.) The formation of myelins is usually an indication that a dilute surfactant phase exists in contact with (concentrated) lamellar phase; i.e., there is a large miscibility gap between the two phases. Thus it is possible that the region labeled "clear" at high electrolyte levels corresponds to a $W + L_\alpha$ region. We did not investigate this matter further because of the additional resources required.

It was noted that the initial formation of L_2 from the solid in the penetration scan (78 °C) was slightly raised (by ca. 1 °C) by the addition of electrolyte. This indicates a slightly decreased solubility of the surfactant at very high concentrations.

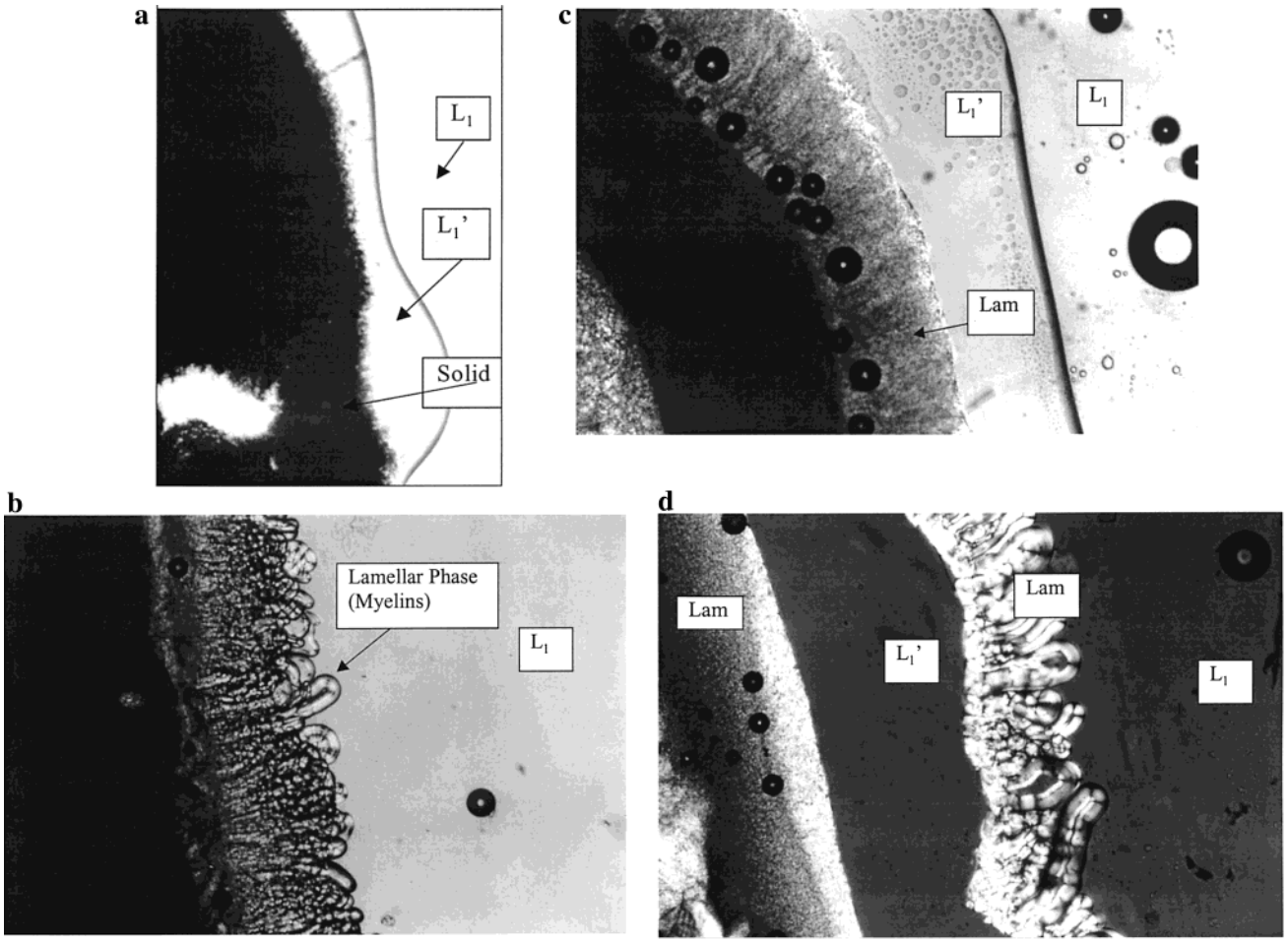

Plate 1. (a) Optical micrograph of the penetration scan of $OCB_{10}NEt_3$ with 1.0 mol dm^{-3} NaCl at 25°C. Surfactant solid on left, solution on right. Magnification ca. ×300. (b) Polarizing optical micrograph of the penetration scan of $OCB_{10}NEt_3$ with 3.0 mol dm^{-3} NaCl at 60 °C. Note myelin formation. Magnification ca. ×300. (c) Polarizing optical micrograph of the penetration scan of $OCB_{10}NEt_3$ with 3.0 mol dm^{-3} NaCl at 90 °C. Note the absence of myelins. Magnification ca. ×300. (d) Polarizing optical micrograph of the penetration scan of $OCB_{10}NEt_3$ with 0.02 mol dm^{-3} NaSCN solution at 50 °C. Note L_1' formed inside lamellar band. Magnification ca. ×300.

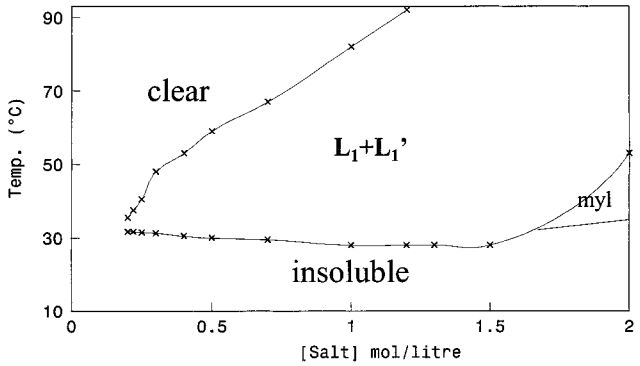

Figure 6. Partial miscibility behavior (temperature range for coexistence of an $L_1 + L_1'$ region as a function of electrolyte concentration) in the OCB-$C_{10}NEt_3/Na_2SO_4$ system. Labels as for Figure 4; myl. indicates formation of lamellar myelins.

Sodium Sulfate Solutions. Surprisingly perhaps, but as with NaCl (and most of the other electrolytes), T_{pen} for the lamellar phase initially decreases with increasing electrolyte concentration, reaching a minimum of 31.9 °C at 0.2 mol dm^{-3} before increasing to 32.7 °C at 1.2 mol dm^{-3}. Above this concentration the lamellar phase first manifests itself in the form of myelins at a temperature lower than that at which the full band of lamellar phase appears. As above with sodium chloride, this may be an indication that a dilute surfactant phase exists in contact with (concentrated) lamellar phase; i.e., there is a large miscibility gap between the two phases. At 1.3 mol dm^{-3} myelins (L_α + W?) are first seen at 32.5 °C, but the full band of lamellar phase does not form until ~41 °C. At 2.0 mol dm^{-3} myelins are present at 32.7 °C.

Partial miscibility is first seen at 0.2 mol dm^{-3} at 32 °C and the LCT decreases to 28 °C at 1.0 mol dm^{-3}. At 2.0 mol dm^{-3} two isotropic phases appear at 53 °C, while myelins are present from 32.7 °C. At concentrations up to ~1.5 mol dm^{-3} the clouding is seen at lower temperatures than the lamellar phase, but thereafter myelin formation precedes clouding. (Figure 6). Thus, above ca. 1.3−1.5 mol dm^{-3}, the partial miscibility loop contacts the lamellar phase at the Krafft boundary; i.e., the concentrated micellar phase L_1' is replaced by L_α. At high electrolyte concentrations the lower part of the miscibility loop always lies below the Krafft boundary. The UCT increases from 48 °C at 0.3 mol dm^{-3} to 92 °C at 1.2 mol dm^{-3} and is above 100 °C at 1.3 mol dm^{-3}.

Sodium Phosphate and Sodium Hydrogen Phosphate Solutions. Neither Na_3PO_4 nor Na_2HPO_4 is very soluble and both have a high degree of water of crystallization. By removing this with heating and subsequently storing the anhydrous salts in a vacuum oven, solutions of up to 0.7mol dm^{-3} can be prepared. This concentration of the electrolytes is insufficient to give changes in T_{pen} values of more than ca. 2 °C, these being similar to those shown in Figure 3 for the other electrolytes.

For the Na_3PO_4 T_{pen} initially decreases with increasing electrolyte concentration reaching a minimum of 31.5 °C at 0.1 mol dm^{-3} and then increases to 33.5 °C at 0.7 mol dm^{-3}. Partial miscibility is first seen at 0.05 mol dm^{-3} at 34 °C, with the LCT decreasing to 28 °C at 0.3 mol dm^{-3} and then increasing to 31.3 °C at 0.7 mol dm^{-3}. The UCT increases from 44 °C at 0.05 mol dm^{-3} to 99 °C at 0.45 mol dm^{-3} (Figure 7).

For Na_2HPO_4 T_{pen} initially decreases with increasing electrolyte concentration reaching a minimum of 32.2 °C at 0.1 mol dm^{-3} and then increases to 33.4 °C at 0.65 mol dm^{-3}. Partial miscibility is first seen at 0.1 mol dm^{-3} at 36.5 °C, decreasing to 32.5 °C at 0.3 mol dm^{-3}, then increasing to 32.3 °C at 0.65 mol dm^{-3}. The upper consolute temperature increases from 38.8 °C at 0.1 mol dm^{-3} to 98 °C at 0.65 mol dm^{-3} (Figure 8).

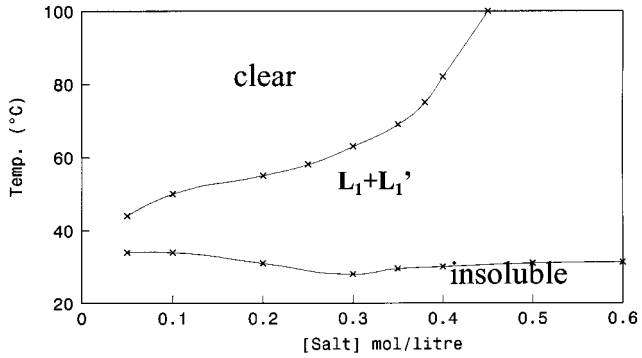

Figure 7. Partial miscibility behavior (temperature range for coexistence of an $L_1 + L_1'$ region as a function of electrolyte concentration) in OCB-$C_{10}NEt_3/Na_3PO_4$ (symbols, see Figure 4).

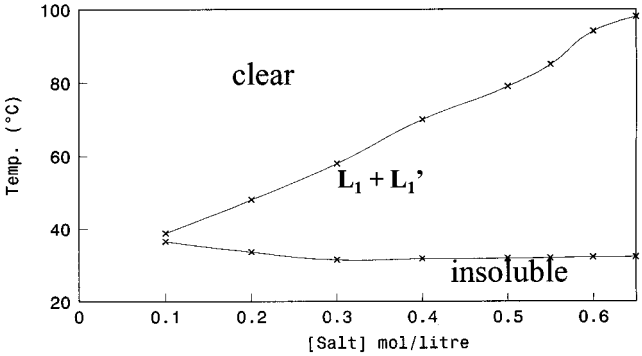

Figure 8. Partial miscibility behavior (temperature range for coexistence of an $L_1 + L_1'$ region as a function of electrolyte concentration) in OCB-$C_{10}NEt_3/Na_2HPO_4$ (symbols, see Figure 4).

Note that in both systems, as with sodium sulfate solutions at higher concentrations, the lower part of the miscibility loop always lies below the Krafft boundary except for the very lowest electrolyte levels where it is observed. However, in these cases the loop does not contact the lamellar phase, possibly because sufficiently high electrolyte concentrations cannot be accessed.

Sodium Thiocyanate Solutions. Due to the hygroscopic nature of NaSCN, the crystals were dried by heating and then stored in a vacuum oven. As with most of the other electrolytes, T_{pen} initially decreases with increasing electrolyte concentration, reaching a minimum of 27.5 °C at 0.02 mol dm^{-3} before increasing to 49 °C at 0.5 mol dm^{-3}. Myelin formation is a frequent occurrence, but in this case it does not indicate the occurrence of L_α + W because no miscibility gap is seen in the micellar region (see below).

There are several differences in behavior from that of other systems, the major one being the occurrence of a "re-entrant" isotropic solution separating two lamellar phase regions (see below). First, at concentrations above 0.03 mol dm^{-3}, the lamellar phase is formed inside a band of solid (i.e., the sequence is $L_1/S/L_\alpha/S$). This re-entrant solid, which presumably is the thiocyanate surfactant salt, dissolves slowly, finally disappearing at 40−45 °C in all samples. Second, there is no indication of clouding (partial miscibility) in any of the phases.

The most remarkable feature of this system is the formation of a second isotropic band (L_1'), which splits the lamellar phase (Figure 9, Plate 1d). The formation of this band is very gradual; thus, at 0.02 mol dm^{-3} it begins forming at 31 °C, and even employing a very slow heating rate (e.g., 0.2 °C min^{-1}) it is not complete until 54 °C. The temperatures at which the L_1'/L_α separation begins and ends both increase with electrolyte

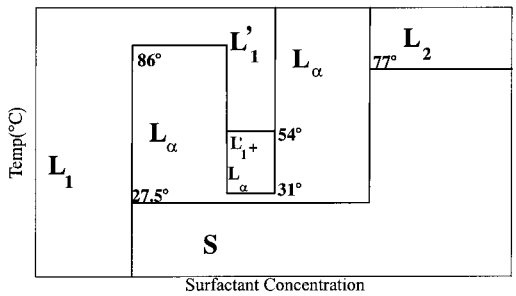

Figure 9. Schematic diagram of penetration scan of OCB-$C_{10}NEt_3$/0.02 M NaSCN.

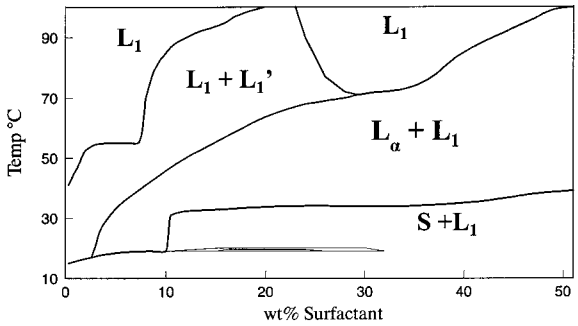

Figure 10. Partial phase diagram of OCB-$C_{10}NEt_3$/1 mol dm^{-3} NaCl. L_1, L_1' represent isotropic liquid phases. For expansion of region between 10 and 35% OCB-$C_{10}NEt_3$ at ca. 20 °C see Figure 11.

concentration. Above 0.06 mol dm^{-3}, the separation is not completed by 100 °C and above 0.2 mol dm^{-3}, no separation is seen at all. In considering these data we must bear in mind that we have a complex, nonequilibrium system with five components present, so multiple phases can coexist over a range of compositions. The phases certainly cannot be represented on a simple binary phase diagram. Nonetheless, the occurrence of an L_1' band within the L_α region does indicate that at and above 0.02 mol dm^{-3} electrolyte, on increasing surfactant concentration, the lamellar phase upper temperature limit increases, then decreases, and then increases again. The initial observation of the L_1' droplets represents the lowest temperature at which L_1'/L_α coexistence region occurs.

While there is less precision in noting the temperature at which the formation of this second isotropic band completely "splits" the lamellar phase, the completion temperature does approximate to the appearance of a single L_1' phase within the L_α region. Moreover, the observation of myelins at the high electrolyte concentrations, without partial miscibility, suggests that the initial surfactant concentration for the formation of lamellar phase is very much reduced.

B. Partial Phase Diagrams. *OCB-$C_{10}NEt_3$ in 1 mol dm^{-3} Sodium Chloride.* In addition to penetration scans, a partial phase diagram of OCB-$C_{10}NEt_3$ in 1 mol dm^{-3} NaCl has been constructed (Figure 10) using about 35 different samples. Both optical microscopy, and observations by eye on sealed samples in a water bath between large polaroid sheets, were employed in its construction. Much of the diagram (Figure 10) shows two-phase regions ($S + L_1$, $L_\alpha + L_1$, and $L_1 + L_1'$). Note that the "step" in the $S + $ iso region at ca. 10% surfactant (see below) is probably a result of the solid changing from the chloride to the bromide salt. Sharp breaks in the other boundaries appear to be valid and may well have the same source (i.e., it is a four-component system, hence multiphase regions are to be expected.). We did not examine the very dilute surfactant part of the diagram in detail. The lamellar phase is first seen (with L_1) at 17 °C at 2.7 wt % OCB-$C_{10}NEt_3$ (cf. 33 °C at 22 wt % in

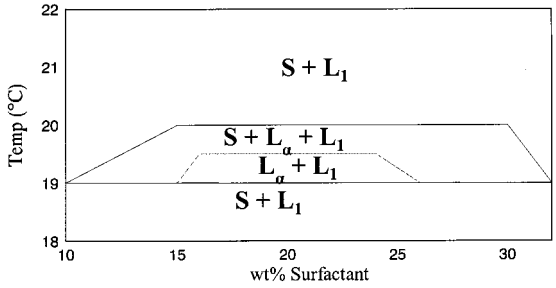

Figure 11. Nonequilibrium portion of OCB-$C_{10}NEt_3$/1 mol dm^{-3} NaCl phase diagram. Behavior observed on heating samples cooled to below 0 °C (symbols as for Figure 10).

water). The melting temperature of the lamellar phase increases fairly linearly with concentration until at 50 wt % OCB-C_{10}-NEt_3 it is still present at 100 °C. (At 50 wt % $OCB_{10}NEt_3$ in water the lamellar phase melts at 84 °C.) A region of partial miscibility exists up to 29.7 wt % OCB-$C_{10}NEt_3$. It is first seen at a concentration as low as 0.3 wt % OCB-$C_{10}NEt_3$, where the solid dissolves to form two isotropic liquids, which on further heating become miscible at 41 °C. This upper miscibility temperature (UCT) initially increases to 56 °C at 3 wt % OCB-$C_{10}NEt_3$ before leveling out until 7.4 wt % when it increases sharply and then curves round until at ~18 wt % the boundary moves above 100 °C and no miscibility is seen. At 23 wt % the miscibility returns and UCT decreases until at 29.7 wt % OCB-$C_{10}NEt_3$ no region of partial miscibility is seen. At this concentration the $L_\alpha + L_1$ region melts to give just one isotropic phase.

As mentioned above, the boundary of regions with S present (the Krafft boundary) increases slowly from 17 to 19 °C at 10 wt % OCB-$C_{10}NEt_3$ and then increases sharply to 31 °C where it remains constant up to 40 wt % before increasing at 45 °C at 52 wt %. In the region below this boundary between 10 and 32 wt % OCB-$C_{10}NEt_3$ we observed significant nonequilibrium behavior (Figure 11). If samples were cooled to well below 0 °C to (mostly) freeze them, and then heated very slowly, at 19 °C the solid begins to dissolve to form lamellar phase. Between 15 and 26 wt % OCB-$C_{10}NEt_3$ all the solid dissolves, but at 19.5 °C a solid reappears. At other concentrations in this region this solid-free area is not observed. At 20 °C the lamellar phase disappears and the $S + L_1$ region is observed again. If a sample is cooled from this region and then reheated, the lamellar phase is not seen until above 20 °C. If, however, the sample is heated until the lamellar phase is formed again and then cooled and reheated, the behavior is as described above. Clearly, the solid initially formed on cooling the lamellar phase below 0 °C is metastable and takes a more stable form on heating through the transient lamellar phase. The metastable solid is probably the chloride salt, while the stable form may well be the bromide.

Note that the sodium chloride and surfactant activities are not constant in any of the two-phase regions on the diagram when the concentration of surfactant is altered. Hence the water content of the lamellar phase may well vary in the area. It is likely to be larger at low surfactant and sodium chloride levels than at high concentrations. Also, at lower OCB-$C_{10}NEt_3$ concentrations there are probably two isotropic phases present in the region labeled $L_\alpha + $ Iso. It was difficult to discern whether there were one or two isotropic regions where both are suspended in a lamellar continuum. The absence of a single lamellar phase region suggests that the water content of this region is less than 50% (at high OCB-$C_{10}NEt_3$ concentrations). As the compositions approached 50% the fraction of isotropic phase is very small.

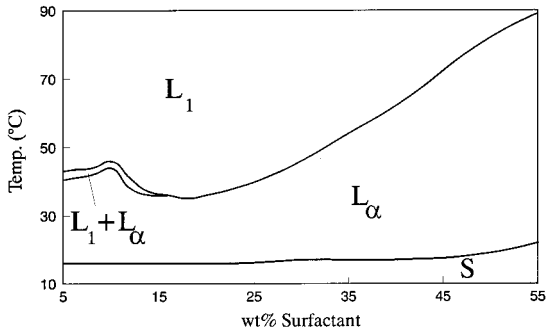

Figure 12. Partial phase diagram of OCB-$C_{10}NEt_3$/0.05 mol dm^{-3} NaSCN system (symbols as for other diagrams).

TABLE 1: Temperatures of Start and Completion of the Re-entrant Isotropic Phase in OCB-$C_{10}NEt_3$/NaSCN System

concn NaSCN (mol dm^{-3})	start temp (°C)	completion temp (°C)
0.02	31	54
0.03	34	72
0.05	54	84
0.06	55	95
0.07	57	>100
0.1	68	>100
0.2	78	>100

OCB-$C_{10}NEt_3$ in 0.05 mol dm^{-3} Sodium Thiocyanate. A partial phase diagram of OCB-$C_{10}NEt_3$ in 0.05 mol dm^{-3} NaSCN has been constructed by observing macroscopic samples through crossed polarizers as above (Figure 12). Concentrations of 5 to 60 wt % OCB-$C_{10}NEt_3$ have investigated (ca. 15 samples).

The phase behavior is much simpler than that seen with NaCl. Between 5 and 16 wt % OCB-$C_{10}NEt_3$, the $L_\alpha \rightarrow L_1$ transition passes through a two-phase region of up to 3 °C wide. This two-phase region becomes narrower until at 16 wt % OCB-$C_{10}NEt_3$ the transition appears to be instantaneous. At 5 wt % OCB-$C_{10}NEt_3$ the $L_\alpha + L_1 \rightarrow L_1$ transition occurs at 40 °C and increases to 46 °C at 10 wt % OCB-$C_{10}NEt_3$. The transition temperature then decreases to a minimum of 35 °C for 18 wt % OCB-$C_{10}NEt_3$. Thus a re-entrant micellar phase is formed (as seen in the penetration scans). The $L_\alpha \rightarrow L_1$ transition temperature then increases rapidly to 89 °C at 55 wt % OCB-$C_{10}NEt_3$, and is greater than 100 °C at 60 wt %. These results confirm both the absence of a partial miscibility loop in this system and that the lamellar phase can occur at considerably lower concentrations in electrolytes than in water.

X-ray Diffraction of OCB-$C_{10}NEt_3$ with Electrolyte Solutions. X-ray diffraction was carried out on a series of lamellar phase samples to determine the influence of electrolytes on the surfactant aggregate dimensions. OCB-$C_{10}NEt_3$ samples were investigated in 1 mol dm^{-3} NaCl, 1 mol dm^{-3} NaBr, and 0.05 mol dm^{-3} and 0.1 mol dm^{-3} NaSCN solutions.

OCB-$C_{10}NEt_3$ with 1 mol dm^{-3} Sodium Chloride. As shown in Figure 10, samples containing below ~50 wt % OCB-$C_{10}NEt_3$ form coexisting regions of lamellar plus an isotropic phase. In Lindemann tubes, the two phases separate out completely under centrifugation. By measuring and comparing the lengths (and thus the volumes) of the two phases, and taking into account their different densities, it is possible to estimate the amount of free electrolyte solution and calculate the concentration of the surfactant in the lamellar phase (see Table 2). The assumption that (almost) all the surfactant is in the mesophase and not partitioned between the mesophase and the aqueous layer has been made. This was confirmed using ^1H NMR of the sample within the Lindemann tube, placed in a standard 5 mm NMR tube. The spectrum of the aqueous layer gave only residual water peak (HDO). Even on increasing the intensity of the spectrum by several factors of 10, there are no signs of any peaks (e.g., the aromatic region). The compositions estimated in this way at ambient laboratory temperature (Table 2) have been assumed to apply at higher temperatures also (up to 60 °C). There was no obvious swelling of the lamellar region at high temperatures to indicate that this assumption was invalid. Also, the time that the samples were left at high temperature was small, and hence any macroscopic variation of composition would also be small, because both water and electrolyte are required to diffuse into the surfactant layer. (The form of the phase diagram at high temperatures, higher miscibility of the surfactant and aqueous regions, makes the loss of water from the aqueous region unlikely.) Any discrepancies would be expected to be most pronounced at low surfactant concentrations and high temperatures. None are obvious in the data presented, which are limited to low temperatures (below 60 °C) for the low concentrations.

TABLE 2: Estimated Lamellar Phase Concentrations (wt % Corrected) for OCB-$C_{10}NEt_3$ in 1 mol dm^{-3} NaCl, As Calculated from the Lengths of Separated Isotropic and Lamellar Phases in Lindemann Tubes

wt %	wt % (corr)	MR[a]	wt %	wt % (corr)	MR[a]
10	17.9	0.0076	40	42.5	0.0258
20	24.7	0.0114	50	50	0.0349
28	33.1	0.0173			

[a] MR is the surfactant/water molar ratio listed so that the data can be compared with NMR results below.

TABLE 3: Dimensions for the Lamellar Phase of the OCB-$C_{10}NEt_3$/1 mol dm^{-3} NaCl System at Various Temperatures from X-ray Measurements

wt % (MR)	temp (°C)	d_0/Å	d_{hc}/Å	d_{aq}/Å	a/Å^2
33.1 (0.0173)	40	85.0	18.8	66.2	59.0
42.5 (0.0258)	40	72.0	20.4	51.6	54.4
50.0 (0.0349)	40	65.7	21.8	43.9	50.8
33.1 (0.0173)	60	75.2	17.3	57.9	67.5
42.5 (0.0258)	60	66.7	19.6	47.1	59.6
50.0 (0.0349)	60	62.2	21.4	40.8	54.6
17.0 (0.0076)	20	118.4	14.2	104.2	78.1
24.7 (0.0114)	30	114.3	18.9	95.4	58.7

Measurements were taken at 40 and 60 °C, while the more dilute samples were run at lower temperatures. From the unit cell spacing, the dimensions of the aqueous and surfactant regions were calculated by standard methods[28] using densities for the surfactant[13] and aqueous[29] regions. These were used to calculate the average surfactant area (a) in the lamellae.[13,28] The data (Table 3) show clearly that the headgroup area decreases at higher concentrations and lower temperatures, as for the system without electrolyte.[13]

OCB-$C_{10}NEt_3$ with 1 mol dm^{-3} Sodium Bromide Solution. Samples containing 30 and 50% OCB-$C_{10}NEt_3$ were examined. These all appeared to be composed of a single lamellar phase (confirmed by NMR, see below). The data (Table 4) show unequivocally that while the headgroup area decreases at higher concentrations and lower temperatures, the values are much smaller than for the system without electrolyte.[13]

OCB-$C_{10}NEt_3$ with 0.05 mol dm^{-3} and 0.1 mol dm^{-3} Sodium Thiocyanate Solutions. Because of the large differences in behavior between sodium thiocyanate and the other electrolytes, a larger number of samples was measured, thus allowing a wider comparison by concentration and temperature. All of the samples

TABLE 4: Dimensions for the Lamellar Phase of OCB-$C_{10}NEt_3$ in 1 mol dm^{-3} NaBr from X-ray Measurements

wt %	temp (°C)	d_0/Å	d_{hc}/Å	d_{aq}/Å	a/Å^2
30	30	102.7	20.9	81.8	53.1
30	40	99.3	20.2	79.1	54.9
30	60	94.2	19.2	75.0	57.9
50	30	73.3	24.7	48.6	45.0
50	40	71.6	24.1	47.5	46.0

TABLE 5: Dimensions for the Lamellar Phase of the OCB-$C_{10}NEt_3$/0.05 mol dm^{-3} NaSCN Solution System from X-ray Scattering Measurements

wt %	MR	temp (°C)	d_0/Å	d_{hc}/Å	d_{aq}/Å	a/Å^2
10	0.0039	30	263	17.0	246	65.2
20	0.0087	30	172	22.3	150	49.7
30	0.0150	30	112	21.7	89.9	51.2
50	0.0349	30	78.0	26.1	51.9	44.7
10	0.0039	40	274	17.7	256	62.5
20	0.0087	40	157	20.4	137	54.4
30	0.0150	40	101.2	19.7	81.5	56.4
50	0.0349	40	72.6	23.5	49.1	49.1
10	0.0039	50	279	18.0	261	61.5
20	0.0087	50	113.0	14.6	98.4	75.8
30	0.0150	60	87.4	17.7	69.7	66.0
50	0.0349	60	64.6	20.9	43.7	53.0

TABLE 6: Dimensions for the Lamellar Phase of OCB-$C_{10}NEt_3$ in 0.1 mol dm^{-3} NaSCN from X-ray Scattering Measurements

wt %	temp(°C)	d_0/Å	d_{hc}/Å	d_{aq}/Å	a/Å^2
30	30	109	21.1	87.5	52.6
30	40	98.6	19.1	79.5	57.9
30	60	87.3	17.0	70.3	65.4
40	30	76.6	24.8	51.8	44.7
40	40	72.6	23.5	49.1	47.2
40	60	65.3	21.1	44.2	52.5

examined were single lamellar phases, again this being confirmed by the NMR measurements (see below). The results (Tables 5 and 6) also confirm that the lamellar phase does occur at much lower concentrations than without electrolyte.

Most of the above data are very similar to those obtained for the other electrolytes, but there are two apparently anomalous results in the calculated values of a. The value decreases with temperature for 10% surfactant in 0.05 mol dm^{-3} NaSCN, while the values for 30 wt % surfactant in 0.05 mol dm^{-3} NaSCN at 30−40 °C are larger than those for 20%. For large values of d_0 (such as in Table 5) the experimental error is larger than for smaller for smaller values, with a difference of one channel number in the measurement of the diffraction peak position making a difference of 2−3 Å. However, this change in d_0 is too small to lead to the anomalous results. In fact, this is the region of the phase diagram where the lamellar phase is much more extensive than in the absence of electrolyte, and hence the "anomalies" do reflect the phase behavior.

^{2}H NMR of OCB-$C_{10}NEt_3$ with Electrolyte Solutions. The ordering of water in the lamellar phase of OCB-$C_{10}NEt_3$ (no electrolyte) was studied previously[13] using deuterium NMR of ^2H_2O to allow the measurement of the quadrupole splittings (Δ). The Δ values are related to the fraction of water molecules bound to heads groups (p_b), and their quadrupole splitting (Δ_b) which is in turn related to their degree of order (S_b). (For more details see ref 30 and the references therein.) If there is a simple chemical equilibrium between surfactant-bound and free water molecules, then Δ is linearly dependent on the surfactant/water mole ratio at low surfactant concentrations, and passes through a maximum when the mole ratio takes the value $n_b - 1$, where n_b is the number of water molecules bound per surfactant. This is not the place to discuss the background to the behavior—a discussion is given in ref 30 and the *Faraday Discuss.* contributions. Suffice to say that, surprising as it may seem, the maximum *is* often observed. Measurements were carried out both as functions of concentration and of temperature. Note that in multiphase samples, overlapping spectra from each present are usually observed. In this study, OCB-$C_{10}NEt_3$ samples were investigated in 1 mol dm^{-3} NaCl, 1 mol dm^{-3} NaBr, and 0.05 mol dm^{-3} NaSCN electrolyte solutions made up with ^2H_2O. Our objective was to confirm that the samples examined by X-rays were single lamellar phases (except where stated otherwise). More importantly, were there changes in the order parameter of the bound water (S_b) that reflected the changes in aggregate structures induced by the addition of electrolyte? For easier comparison of the results with and without electrolyte, we include a table of the data for the OCB-$C_{10}NEt_3$/water system, the data being taken from ref 13 (Table 7).

TABLE 7: ^{2}H Quadrupole Splittings for the Lamellar Phase of the OCB-$C_{10}NEt_3$/^2H_2O System at 30 and 50 °C (Data from Ref 13)

	Δ (Hz)			Δ (Hz)	
mole ratio	30 °C	50 °C	mole ratio	30 °C	50 °C
0.0151	198	isotropic	0.0660	1067	717
0.0180	258	isotropic	0.0949	1411	965
0.0224	363	195	0.1150	1750	1250
0.0317	501	286	0.1255	2039	1495
0.0345	576	352	0.1754	1994	1881
0.0405	632	396	0.2196	1800	2130
0.0551	852	566	0.2842	1826	2670

OCB-$C_{10}NEt_3$ with 1 mol dm^{-3} Sodium Chloride. Figure 13 shows a typical NMR spectrum of OCB-$C_{10}NEt_3$/NaCl mixture in the $L_1 + L_\alpha$ two-phase region. The middle peak is due to the isotropic phase, and the quarupole splitting is measured between the outer peaks. Note that this is a sample where the lamellar phase is aligned with the axis along the magnetic field, hence Δ is actually half of the observed splitting. As in the absence of electrolyte,[13] we frequently observed sample alignment.

A range of concentrations was examined at a series of temperatures (Figure 14). Since the observed Δ value is proportional to the surfactant/water molar ratio, we include this parameter in the table of data to facilitate comparison. It is clear that, while the Δ values are similar to those without electrolyte at the very highest concentrations, they are usually larger in samples containing NaCl at other concentrations. This applies equally to samples where an isotropic phase certainly is present (15%) and ones where it certainly is not (69%). Thus addition of NaCl has increased the Δ values. Since electrolyte would be expected to compete for bound water with the headgroups it is unlikely to increase Δ by increasing the bound fraction (p_b). The obvious explanation for the increase is that S_b, the order parameter of the bound water, increases. This is exactly what would be expected from the change in a deduced from the X-ray measurements. The dramatic reduction Δ with increasing temperature then indicates that a increases, again consistent with X-ray data.

As a minor point, note that there is no maximum in the dependence of Δ on concentration at lower temperature for any of the electrolyte systems, although the maximum is observed for the samples without salt. One expects added electrolytes to compete with headgroups for the binding of water, hence this absence is not a surprise.

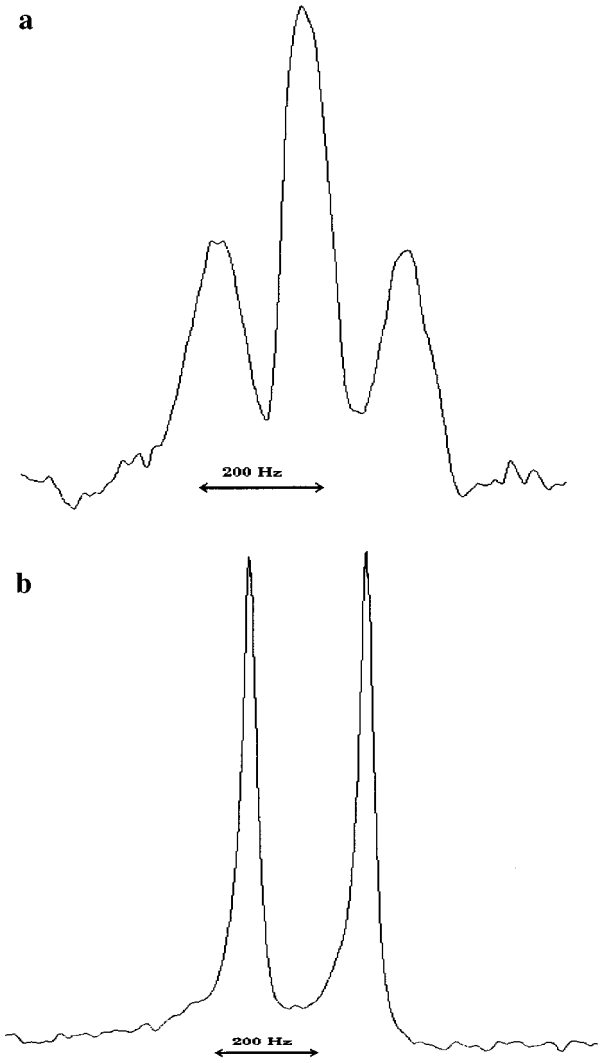

Figure 13. (a) ^{2}H NMR spectrum of 15 wt % OCB-$C_{10}NEt_3$ in 1 mol dm^{-3} NaCl at 30 °C. (b) ^{2}H NMR spectrum of 15 wt % C-10 in 0.05 M NaSCN at 30 °C.

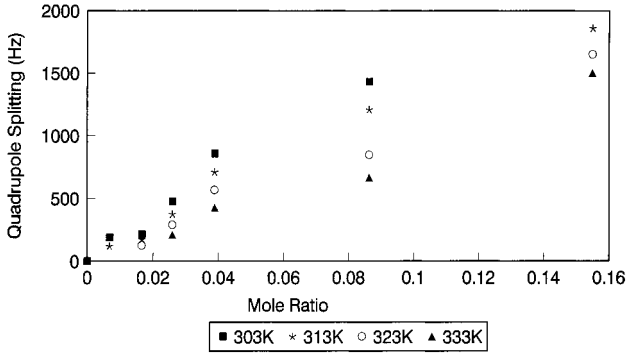

Figure 14. Plot of ^{2}H quadrupole splitting (△) versus surfactant/water mole ratio for OCB-$C_{10}NEt_3$ in 1 mol dm^{-3} NaCl solution.

OCB-$C_{10}NEt_3$ with 1 mol dm^{-3} Sodium Bromide. Again, a range of concentrations was examined over a series of temperatures. In this case the occurrence of lamellar + isotropic spectra was rare. The Δ values are larger than in water alone.

OCB-$C_{10}NEt_3$ with 0.05 mol dm^{-3} Sodium Thiocyanate. The data for these samples are shown in Figures 18 and 19 while a spectrum is shown in Figure 13b. Again the Δ values are larger than without electrolyte, and Figure 13b is a spectrum typical of a single lamellar phase with the director aligned within (along) the magnetic field of the spectrometer.

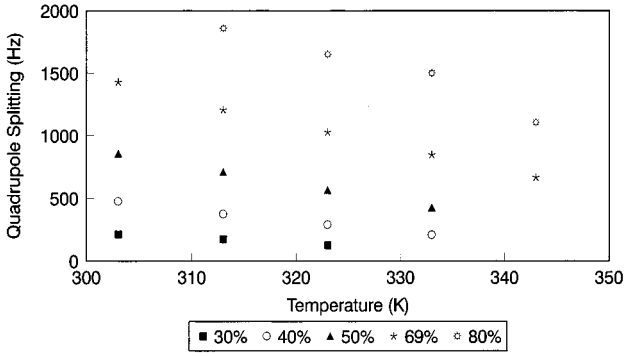

Figure 15. Plot of ^{2}H quadrupole splitting (△) versus temperature for OCB-$C_{10}NEt_3$ in 1 mol dm^{-3} NaCl solution.

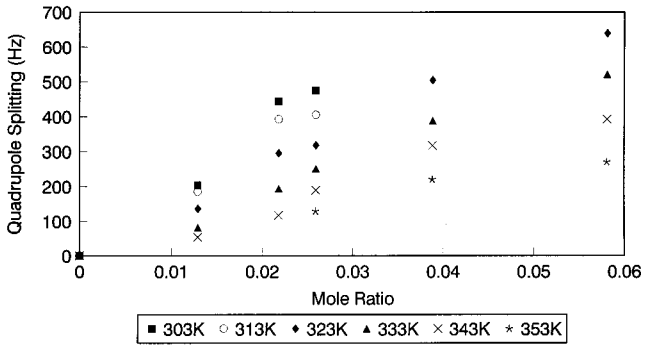

Figure 16. Plot of ^{2}H quadrupole splitting (△) versus mole ratio for OCB-$C_{10}NEt_3$ in 1 mol dm^{-3} NaBr solution.

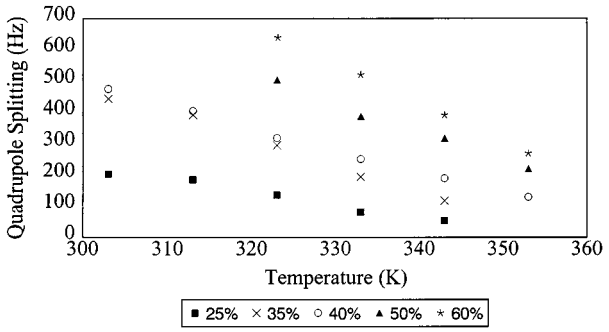

Figure 17. Plot of ^{2}H quadrupole splitting (△) versus temperature for OCB-$C_{10}NEt_3$ in 1 mol dm^{-3} NaBr solution.

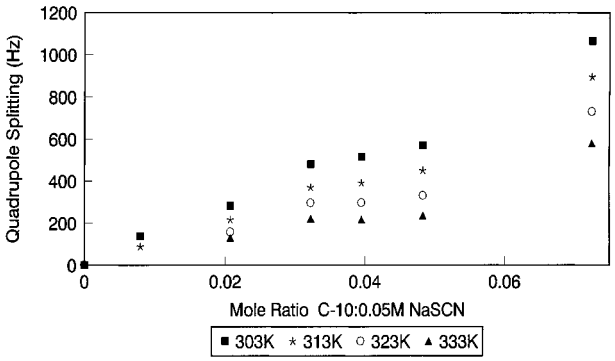

Figure 18. Plot of ^{2}H quadrupole splitting (△) versus mole ratio for for OCB-$C_{10}NEt_3$ in 0.05 mol dm^{-3} NaSCN solution.

Discussion

Phase Behavior. The penetration scans with electrolyte solutions show two main phenomena: an initial change (usually a reduction) in the penetration temperature of the lamellar phase and the existence of a region of partial miscibility (except for

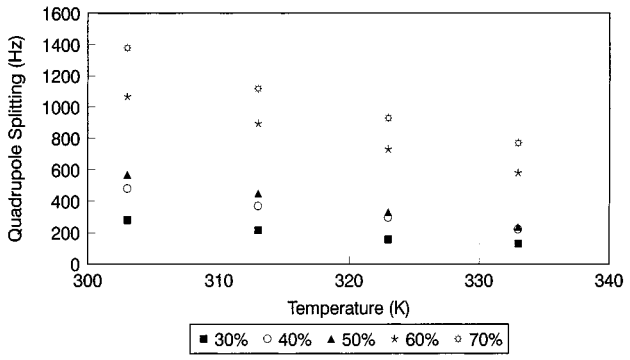

Figure 19. Plot of ^2H quadrupole splitting (△) versus temperature for OCB-$C_{10}NEt_3$ in 0.05 mol dm^{-3} NaSCN solution.

NaSCN which has a re-entrant micellar phase instead). Although the two follow a similar trend, they are quite different transitions. The solubility of the solid in the aqueous electrolyte determines T_{pen} and involves large change in enthalpy because of the large change in solute mobility on dissolution. Clouding is due to a liquid−liquid phase transition which involve much smaller transition enthalpies. Hence the latter is far more influenced by added solute because like "freezing point lowering" of a solvent by nonvolatile solutes, the change in transition temperature is inversely related to the transition enthalpy.

The variations in T_{pen} simply reflect the ease of packing in the surfactant crystal. All the electrolytes except NaBr lower $T_{pen,}$ which indicates a less effective packing of the anions than that for bromide. At first sight this is surprising for the multivalent counterions, but they *are* much more bulky. However, most of the effects are small, and will also be influenced to some extent by the fact that the solutions contain mixed counterions (which increases surfactant solubility).

That the reduction in penetration temperature *is* due to counterion exchange, with the occurrence of, e.g. OCB-$C_{10}NEt_3$ chloride and OCB-$C_{10}NEt_3$ sulfate which have greater solubilities and lower penetration temperatures, has been briefly investigated. These two compounds were prepared by using an anionic exchange resin (Duolite 113(C1) containing a quaternary ammonium functional group) pretreated with the appropriate electrolyte. Penetration scans were carried out on them with water, and gave approximate lamellar phase penetration of 11.5 and 5 °C, respectively.

This reduction in penetration temperature is not seen in NaBr solution due to the common ion effect. This states that when a soluble salt (NaBr) has an ion in common with a sparingly soluble salt (OCB-$C_{10}NEt_3$ with a bromide counterion), the solubility of the less soluble salt is decreased even further. The addition of NaBr increases the concentration of the cation, and so pushes the equilibrium

$$\text{OCB-}C_{10}NEt_3Br(s) \leftrightarrow \text{OCB-}C_{10}NE_3^{+}(aq) + Br^{-}(aq)$$

further to the left-hand side thus precipitating OCB-$C_{10}NEt_3$. As electrolyte concentration increases, a higher temperature is required to reach the concentration of OCB-$C_{10}NEt_3$ for the formation of the lamellar phase.

The large differences in partial miscibility induced by the different electrolytes are important practically because of their potential applications in general product formulation. Note that the actual changes in micelle and liquid crystal structures are small. None of the electrolytes change the lamellar phase to other liquid crystals. They simply modify the boundaries.

The minimum electrolyte concentration for the initial occurrence of clouding is roughly similar (0.06−0.2 M) for all the electrolytes (except NaSCN). Clearly, the major effect is screening of the intermicellar electrostatic repulsion. It is noticeable that higher concentrations of the multivalent electrolytes are required to induce clouding than for univalent electrolytes. This is the opposite order to their ionic strength. But the differences between the electrolytes probably also reflect the differing degrees of specific anion−headgroup interactions, which influence both micelle size and charge. Highly charged polyoxy anions generally are not adsorbed at surfaces while polarizable anions are. It would appear that a small binding of anions (with chloride and bromide) can promote clouding. Larger binding, as we expect with thiocyanate, clearly has the opposite effect! Note that bromide at high concentrations "salts-in", because the LCT moves above 100 °C, while there is no sign of this with the polyoxy anions. All of these observations are consistent with the known "Hofmeister series" behavior of the electrolytes. They are all consistent with known adsorption/desorption properties of the anions. We do not need to resort to "water structure" to account for the observations.

The most difficult observations to understand are the behavior of the system with NaSCN. Here the absence of clouding is expected because this electrolyte salts-in. But the re-entrant isotropic phase, and the presence of the lamellar phase at low concentrations, indicate opposing effects. The occurrence of a "disordered" solution implies small noninteracting (or weakly interacting) micelles, while the presence of a mesophase implies large, strongly interacting micelles. One hypothesis to account for this might be the existence of water structure, but we preferred to carry out more experiments to obtain direct evidence of structural changes (see below).

A final comment in this section concerns the absence of the two-lamellar phase coexistence that occurs[4] in the *gemini* surfactant analogues OCB-$C_{10}NEt_3$. Given the range of systems examined, it seems likely that if this behavior did occur, we would have observed it. The most obvious difference between the two surfactants is the gemini/nongemini feature. But since this does not interfere with other partial miscibility behavior,[31] it might be ruled out here. So we suspect that the headgroup structure is involved. Alteration of the trimethylammonium group to a triethylammonium group changes the headgroup volume by about a factor of 2, which must influence the bromide ion location. This would appear to be a fruitful line of investigation to follow the matter further.

X-ray Diffraction. X-ray diffraction has been used to show the effect of the various electrolytes on the dimensions of the lamellar phase of OCB-$C_{10}NEt_3$. Note that the densities of the electrolyte solutions differ slightly from that of water, so exact matching of liquid crystal dimensions in samples with identical weight proportions of surfactant is not expected. The effect of electrolyte may be looked at by comparing the dimensions of the lamellar phase at a standard surfactant concentration and temperature (e.g., 30% and 50 wt % OCB-$C_{10}NEt_3$ at 40 °C, Table 8).

It can be seen that there is very little effect on the lamellar structure when water is replaced by 1 mol dm^{-3} NaCl solution, whereas there is an increase in d_0 with 1 mol dm^{-3} NaBr and with the NaSCN solutions which also results in an increase in hydrocarbon thickness and a reduction in area per headgroup. The initial addition of the low level (0.05 mol dm^{-3}) of NaSCN gives a large reduction in the *a* value, but increasing the concentration from 0.5 to 0.1 mol dm^{-3} appears to have very little further effect. The reduction would be expected to result in la-

TABLE 8: Dimensions of the Lamellar Phase for OCB-$C_{10}NEt_3$ in Various Solutions at 40 °C from X-ray Scattering Measurements

wt %	solvent	d_0 (Å)	d_{hc} (Å)	a (Å^2)
30	H_2O	89.1	17.3	64.1
30	1 mol dm^{-3} NaCl	89[a]	18.0	62.2
30	1 mol dm^{-3} NaBr	99.3	20.2	54.9
30	0.05 mol dm^{-3} NaSCN	101.2	19.7	56.4
30	0.1 mol dm^{-3} NaSCN	98.6	19.1	57.9
50	H_2O	66.6	21.6	51.4
50	1 mol dm^{-3} NaCl	65.7	21.8	50.8
50	1 mol dm^{-3} NaBr	71.6	24.1	46.0
50	0.05 mol dm^{-3} NaSCN	72.6	23.5	49.1
50	0.1 mol dm^{-3} NaSCN	72.6	23.5	47.2

[a] Interpolated value.

TABLE 9: ^{2}H Quadrupole Splittings (Hz) for the Lamellar Phase of OCB-$C_{10}NEt_3$ in Different Systems

wt %	system	303 K	313 K	323 K	323 K
30	D_2O	230	170		
30	1 M NaCl	212	172	124	
30	1 M NaBr	423	380	283	
30	0.05 M NaSCN	276	202	138	
40	D_2O	400	302	225	
40	1 M NaCl	475	373	288	
40	1 M NaBr	475	405	318	
40	0.05 M NaSCN	481	370	296	
50	D_2O	590	490	395	305
50	1 M NaCl	856	709	566	426
50	1 M NaBr			504	388
50	0.05 M NaSCN	650	530	420	330

mellar phase formation at lower concentrations, just as is observed.

^{2}H NMR. The ^{2}H quadrupole splittings change with the fraction of bound water and its order parameter. If the area per headgroup increases, then the order parameter of bound water is expected to decrease and visa versa. All of the systems show a roughly linear dependence of Δ on surfactant/water molar ratio in the composition region studied, as expected. Again, similar to the behavior in water, there is a sharp decrease in Δ with increasing temperature. Differences between the electrolytes become clearer when the data are listed, as in tables. From these it is clear that Δ is larger in the electrolyte solutions, even with 0.05 mol dm^{-3} NaSCN. This confirms the conclusions drawn from X-ray data that the changes in mesophase behavior induced by the electrolytes arise from changes in aggregate structures, specifically a reduction in the value of a. It is tempting to attribute the largest increase in Δ, which which occurs with NaBr, to the largest decrease in the value of a. But X-ray data show that NaSCN at 0.05 mol dm^{-3} gives a similar a value to that observed with NaBr. Hence it would appear that there is some additional process occurring with the latter electrolyte (see below). At very high surfactant concentrations (> ca. 65%) there is more bound than free water present, and given the possibility for water to be bound at a number of sites, each with a different Δ_b value and different binding strengths, the variation of Δ with both temperatures and concentration is likely to be complex. This would be expected to obscure the maximum in Δ vs concentration observed for the electrolyte-free system.

Unusual Behavior of OCB-$C_{10}NEt_3$ with NaSCN. The reappearance of the lamellar phase with NaSCN at low surfactant concentrations is unexpected. There is no doubt that the SCN ions adsorb to the micelle surface and reduce the a value. At the surfactant concentration employed the overall ionic strength is of the order of 0.1 mol dm^{-3}, hence the debye length is at least 10 Å. This means that the interheadgroup electrostatic interactions are still present in the system. Indeed, the concentration of surfactant (ca. 0.1 mol dm^{-3}) is much in excess of the added electrolyte, so that even if all the added anions are bound at the micelle surface, there is still an excess of surfactant charge. The simple adsorption of the SCN ions would not be expected to give a lamellar phase at low concentrations. In previous papers we have attributed the occurrence of lamellar instead of hexagonal or other phases with these amphitropic surfactants to the tendency for self-association of the OCB units within the micelle interior, rather than occupying surface sites. It would appear that SCN ions displace the OCB groups from the surface to the micelle interior. If this is the case, then NaSCN should increase the solubility of thermotropic mesogens in the system. As this was a major objective of the present study, it is certainly worth pursuing in the future.

Acknowledgment. We thank the SERC (now EPSRC) and the University of Salford for financial support, and SERC (now CLRC) Daresbury laboratory for the X-ray facilities.

References and Notes

(1) Kunitake, T. *Angew. Chem., Int. Ed. Engl.* **1992**, *31*, 709.
(2) Navarro-Rodriguez, D.; Frere, Y.; Gramain, P.; Guillon, D.; Skoulios, A. *Liq. Cryst.* **1991**, *9*, 321.
(3) Corcoran, J.; Fuller, S.; Rahman, R.; Shinde, N.; Tiddy, G. J. T.; Attard, G. S. *J. Mater. Chem.* **1992**, *2*, 695.
(4) Fuller, S.; Hopwood, J.; Rahman, R.; Shinde, N.; Tiddy, G. J. T.; Attard, G. S.; Howell, O.; Sproston, S. *Liq. Cryst.* **1992**, *12*, 521.
(5) Fuller, S.; Shinde, N.; Tiddy, G. J. T.; Attard, G. S.; Howell, O. *Langmuir* **1996**, *12*, 1117.
(6) Neumann, B.; Sauer, C.; Diele, S.; Tschierske, C. *J. Mater. Chem.* **1996**, *6*, 1087.
(7) Lindner, N.; Kölbel, M.; Sauer, C.; Diele, S.; Jokiranta, J.; Tschierske, C. *J. Phys. Chem. B.* **1998**, *102*, 5261.
(8) Lattermann, G.; Staufer, G. *Liq. Cryst.* **1989**, *4*, 347.
(9) Brezesinski, G.; Mädicke, A.; Tschierske, C.; Zaschke, H.; Kuschel, F. *Mol. Cryst. Liq. Cryst. Lett.* **1988**, *5*, 155.
(10) Diele, S.; Mädicke, A.; Geissler, E.; Meinel, K.; Demus, D.; Sackmann, H. *Mol. Cryst. Liq. Cryst.* **1989**, *166*, 131.
(11) Everaars, M. D.; Marcelis, A. T. M.; Sudhölter, E. J. R. *Langmuir* **1993**, *9*, 1986.
(12) Tiddy, G. J. T.; Fuller, S.; Zana, R., et al., unpublished results.
(13) Attard, G. S.; Fuller, S.; Howell O.; Tiddy, G. J. T. *Langmuir*, in press.
(14) Blackmore, E. S.; Tiddy, G. J. T.; *J. Chem. Soc., Faraday Trans. 2* **1988** *84*, 1115.
(15) Holmes, M. C.; Smith, A. M.; Leaver, M. S. *J. Phys. II* **1993**, *3*, 1357.
(16) Leaver, M. S.; Holmes, M. C. *J. Phys. II* **1993**, *3*, 105.
(17) Holmes, M. C.; Leave, M. S.; Smith, A. M., *Langmuir* **1995**, ***11***, 356.
(18) Funari, S. S.; Holmes, M. C.; Tiddy, G. J. T. *J. Phys. Chem*. **1992**, *96*, 11029.
(19) Fairhurst, C. E.; Holmes, M. C.; Leaver, M. S. *Langmuir* **1996**, *12*, 6336.
(20) Burgoyne, J.; Holmes, M. C.; Tiddy, G. J. T. *J. Phys. Chem.* **1995**, *99*, 6054.
(21) Holmes, M. C. *Curr. Opin. Colloid Interface Sci.* **1998**, *3*, 485.
(22) McBain, J. W.; Burnett, A. J. *J. Chem. Soc.* **1922**, *121*, 1320.
(23) McBain J. W., Lazarus L. H.; Pitter, A. V. *Z. Phys. Chem.* **1926**, *A147*, 87.
(24) Laughlin, R. G. *The Aqueous Phase Behaviour of Surfactants*; Academic Press: London, 1994; pp 377−83 and 422−451.
(25) Conroy, J. P.; Hall, C.; Leng, C. A.; Rendall, K.; Tiddy, G. J. T.; Walsh, J.; Lindblom, G. *Prog. Colloid Polym. Sci.* **1990**, *82*, 253.
(26) Lawrence, A. S. C. In *Surface Activity and Detergency*; Durham, K., Ed.; MacMillan: 1961; p 158.
(27) Lawrence, A. S. C.; Bingham, A.; Capper, C. B.; Hulme, K. *J. Phys Chem.* **1964**, *68*, 3470.
(28) Luzzati, V. In *Biological Membranes*; Chapman, D., Wallach, D. H. F., Eds.; Academic Press: New York, 1978; p 71.
(29) *CRC Handbook of Chemistry and Physics*; CRC Press: Cleveland, OH, 1974.
(30) Carvell, M.; Hall, D. G.; Lyle, I. G.; Tiddy, G. J. T. *Faraday Discuss. Chem Soc*. **1986**, *81*, 223.
(31) Fuller S.; Tiddy G. J. T.; Zana R., unpublished results.